The influence of inorganic dopants on the electrochemical performance of polyaniline-based composites

Okechukwu Benjamin Okafor[1*], *Abimbola Patricia Idowu* Popoola [1†] , and *Olawale Muhamed* Popoola [2], and *Ngcwangu* Sinako[1]

[1]Chemical, Metallurgical and Materials Engineering Department Tshwane University of Technology, Pretoria, South Africa
[2]Electrical Engineering Department, Tshwane University of Technology, Pretoria, South Africa

Abstract. The study investigates the influence of different inorganic acid dopants on the electrochemical performance of polyaniline/reduced graphene oxide (PANI/rGO) nanocomposite supercapacitor electrode. The nanocomposites were synthesized by in-situ oxidation of aniline using ammonium persulfate (APS) as the oxidizing agent in different inorganic acids. The electrochemical performance of the electrodes fabricated using different acid-doped PANI/rGO nanocomposites was characterized in 1 M $NaSO_4$ electrolyte using cyclic voltammetry (CV), electrochemical impedance spectroscopy (EIS) and galvanostatic charge-discharge (GCD) test. The HCl-doped PANI/rGO electrode delivered the maximum specific capacitance of 207 Fg^{-1} at a current density of 0.2 Ag^{-1}, which shows the high efficiency of the material. The HNO_3-doped PANI/rGO electrode gave the least capacitance of 50.3 Fg^{-1} at the same current density. The structural analysis was done by X-ray diffraction, scanning electron microscopy (SEM) and Fourier transform infrared (FTIR).

1 Introduction

A combination of population, technological and economic advancements has led to an increase in energy demands and energy storage systems. The invention of energy storage systems such as supercapacitors has shown to be a great deal in the stabilization of the grid, use in electric vehicles and portable electronic devices. Since the discovery of conducting polymers (CPs) in 1977, many researchers have been interested in exploring their outstanding properties and potential applications in sensors, memory devices, and energy storage systems (ESS) [1]. CPs have good electrical properties, flexibility, low cost and are easy to synthesize. In a supercapacitor device, CPs are employed as electrode material that stores charge through a rapid, reversible redox process. Amongst the many CPs, polyaniline (PANI) has been considered greatly as a fascinating energy storage material because of its unique structure, light weight, high conductivity, and high specific capacitance. Studies have shown

* Okechukwu B. Okafor: mrbengeneral@gmail.com

that the introduction of dopants is used to modify the structure and electrochemical properties of PANI-based electrodes [2]. The introduction of dopants during polymerization enhances the protonation of aniline. However, the use of PANI as an electrode material in ESS has been limited by the degradation of PANI after many repeated charging/discharging cycles [3]. Graphene is a nanostructured form of carbon with unique mechanical, electrical, and light-weight properties and chemical stability, which has been explored as an electrode material. They store charge via electrostatic interaction that takes place at the electrode/electrolyte interface [4]. The nanocomposite of PANI and reduced graphene utilized as an electrode delivers improved electrochemical performance. This study will investigate the effect of different inorganic acids (HCl, H_2SO_4, H_3PO_4 and HNO_3) on the electrochemical behaviour of PANI/rGO nanocomposite synthesized by chemical oxidation polymerization.

2 Materials and methodology

2.1 Materials

Reduced graphene oxide nanopowder, aniline, ammonium persulfate $(NH_4)_2S_2O_8$ (APS), hydrochloric acid (HCl), nitric acid (HNO_3), phosphoric acid (H_3PO_4), sulfuric acid (H_2SO_4), sodium sulphate, ethanol, acetone, distilled water, N-Methyl-2-pyrrolidone (NMP) and Polyvinylidene Fluoride (PVDF).

2.2 Preparation of nanocomposite

The acid-doped PANI/rGO nanocomposites were synthesized by chemical oxidation polymerization in the presence of different inorganic acids using a synthesis method adopted from Verma and coworkers [5]. 5 ml of pre-cooled aniline were poured into a beaker containing 20ml 1 M HCl and stirred for 30 minutes until a clear solution was formed. 15.6g of APS powder was dissolved in a separate beaker containing 50 ml of deionized water for about 1 hour. A third beaker was used to disperse reduced graphene oxide in deionized water using an ultrasonicator for an hour. The dispersed reduced graphene was then transferred into aniline-HCl solution while still stirring. Thereafter, the APS solution was then added dropwise into the beaker containing rGO + aniline-HCl and stirred continuously in an ice bath using a magnetic stirrer until the overall mixture turned dark green. The mixture is placed in a refrigerator for about 6 hours. Lastly, the resulting mixture was washed, dried and crushed to have the HCl-doped PANI/rGO nanocomposite designated as PR-C. Similar procedures were used for the preparation of PANI/rGO doped with HNO_3, H_3PO_4, and H_2SO_4, designated as PR-N, PR-P and PR-S, respectively.

2.2.1 Preparation of PANI-rGO nanocomposite electrode

The polymer nanocomposite electrode was fabricated by combining the active material (PANI-PGO nanocomposite), conductive carbon black, and PVDF binder in an 80:10:10 weight ratio using a mortar. After adding three drops of NMP solvent, the mixture was well mixed with a pestle to create a homogenous slurry. This slurry was then brush-coated onto a 1 cm^2 area of nickel foam. After coating, the nickel foam kept drying overnight in an oven at 60°C. The final electrode material used for electrochemical testing had a mass of 2.5 mg.

2.3 Material characterization

XRD analysis of the prepared samples was conducted using a X' pert PRO X-ray diffractometer (PANalytical, United Kingdom) equipped with a Cu Kα radiation source (λ = 0.1542 nm) at 25 ºC. The phase structures of the synthesized samples were examined in reflection mode over a 2θ range of 10–80. For the structural analysis Zeiss Ultra Plus 55 field-emission scanning electron microscope (FESEM, Japan) operating at an accelerating voltage of 2.0 kV was used. To determine the electrochemical properties, the fabricated PANI/rGO composite electrode was characterized using the 3-electrode system with PGSTAT302N electrochemical workstation in 1M $NaSO_4$ electrolyte. Cyclic voltammetry (CV) measurement was done at different scan rates from 5 to 100 mVs^{-1} at a voltage window from -0.2 to 0.7V. Galvanostatic charge-discharge (GCD) was conducted by charging and discharging the working electrode using current densities of 0.5 to 5 Ag^{-1}. Electrochemical impedance spectroscopy (EIS) measurement was conducted in the frequency range from 0.001 Hz to 100 kHz, with an AC amplitude of 5 mV.

3 Results and discussion

3.1 Spectra characterization

FTIR: Figure 1a shows the FTIR spectra of the synthesized PANI/rGO nanocomposite with different inorganic acid dopants. All samples exhibit the characteristic bands of doped polyaniline: a strong peak in the 1550–1600 cm^{-1} region from quinoid ring C=C stretching. PR-C shows the highest quinoid peak at 1590 cm^{-1} compared to other acid-doped composites. This shows a stronger π-π interaction between the conducting PANI and the π bond of rGO. The characteristic peak near 1480 cm^{-1} stands for the benzenoid ring C=C vibrations. A distinct feature observed approximately between 1250–1300 cm^{-1} for all the doped composites corresponds to the C–N stretching mode of aromatic amine units in PANI [6, 7]. All acid-doped composite spectra show a pronounced absorption in the ~1100 cm^{-1} vibration, which is attributed to the delocalized polaron $C–N^+$ vibration, which is a characteristic of a conductive form of PANI (emeraldine salt). Comparing the different spectra, differences in peak intensities and slight shifts reflect varying protonation levels and bonding induced by the different inorganic acid dopants. The PR-S composite shows the most intense peak ~1100 cm^{-1} relative to its quinoid/benzenoid bands, indicating that a high degree of protonation is achieved by a stronger acid (H_2SO_4). Phosphoric acid-doped composite is a weaker acid and shows a low protonation level. The PR-N spectrum also reveals a minor band near ~1384 cm^{-1}, which can be attributed to N–O stretching of residual NO_3^-. Therefore, it was revealed that the more highly protonated PANI shows improved polaronic peak and anion bands, and it is produced by a stronger acid than a weaker inorganic acid [8]. The obvious peaks of PANI in the PANI/rGO composite suggest a well-wrapped PANI on the rGO. The different spectra revealed the molecular interaction with different organic acids and a strong π-π interaction between the conducting PANI and the π bond of rGO.

XRD: The XRD patterns of PANI/rGO doped with different inorganic acids are presented in Figure 1b. In all samples, the characteristic PANI emeraldine salt diffraction features in the ~19.5 – 25° region are observed, confirming the formation of PANI and that their crystallinity was retained after the formation of the nanocomposites [9]. PR-C, PR-N show a sharp diffraction peak at ~2θ = 25° and 26 °, respectively, indicating a semi-crystalline PANI structure. In contrast, PR-P displays only a broad, low-intensity diffraction hump around 2θ ≈ 20–25° with no distinct peak, signifying predominantly amorphous polymer content [7]. PR-S shows two discernible peaks at approximately 20° and 25°, implying the presence of multiple ordered reflections. Notably, the peak at 2θ ~25° feature can be attributed to the

periodicity of PANI chains overlapping with the (002) graphitic plane of rGO, while the ~20° feature corresponds to inter-chain spacing in the polymer [10]. The relative sharpness and intensity of these peaks increase in the order ≈ PR-P > PR-S > PR-N > PR-C, which correlates with average crystallite size. A previous study has reported that the weaker acid strength of H_3PO_4 likely leads to incomplete protonation of PANI, further contributing to the diminished structural order observed in PR-P. HCl-doped PANI exhibits higher crystallinity and conductivity than PANI doped with H_2SO_4 or H_3PO_4 [11].

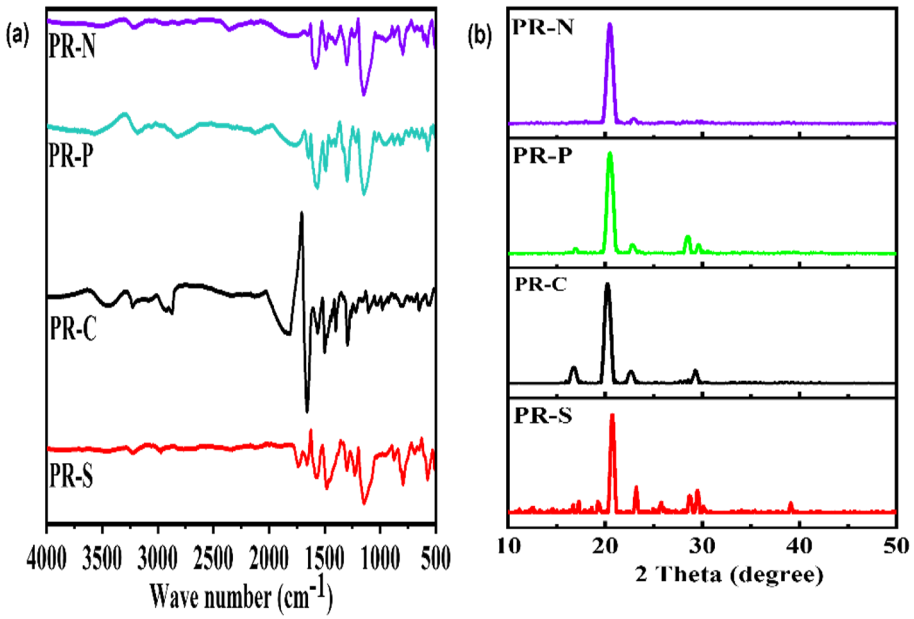

Fig. 1. (a) FTIR spectrum and (b) XRD spectrum of PR-N, PR-C, PR-P and PR-S nanocomposite electrode.

3.2 Microstructure characterization

Figure 2a–d shows the surface morphology of different acid-doped PANI/rGO composites, as examined by SEM. All acid-doped PANI/rGO composite samples (PR-S, PR-P, PR-C, PR-N) exhibit distinct surface morphologies, reflecting the influence of the acid dopant. The PR-S shows a highly porous, fibrous network with minimal agglomeration. H_3PO_4-doped sample (PR-P) presents compact, globular aggregates, indicating lower porosity and increased particle agglomeration. The HCl-doped composite (PR-C) features nanofiber-like PANI structures that form an interconnected coating across the rGO sheets. Meanwhile, nitric acid doping (PR-N) yields extended polymer structures (reported as sheet-like deposits or elongated nanotubes) covering the graphene support [12]. These morphological differences directly impact electrical and electrochemical performance [13]. A fibrous, open architecture (as in PR-S and PR-C) provides high surface area and continuous conductive pathways, enhancing charge transport and pseudocapacitive activity [14]. In contrast, the agglomerated morphology of PR-P seen in the micrograph will likely impede electrolyte access and electron transport, aligning with reports by Tursun et al. of reduced conductivity in bulky phosphate-doped PANI [11]. By adjusting the acid dopant, the PANI/rGO microstructure may be controlled, which in turn allows the electronic conductivity and electrochemical properties of the composite to be tuned. Figure 3(a-d) presents the energy-dispersed spectroscopy (EDS) showing the elemental percentage composition of all the

nanocomposites doped with different inorganic acids. Carbon, oxygen, nitrogen and sulfur can be observed from the spectrum, which confirms the constituents of the PANI/rGO nanocomposite. From the EDS, the presence of the inorganic acids used in each dopant can be confirmed.

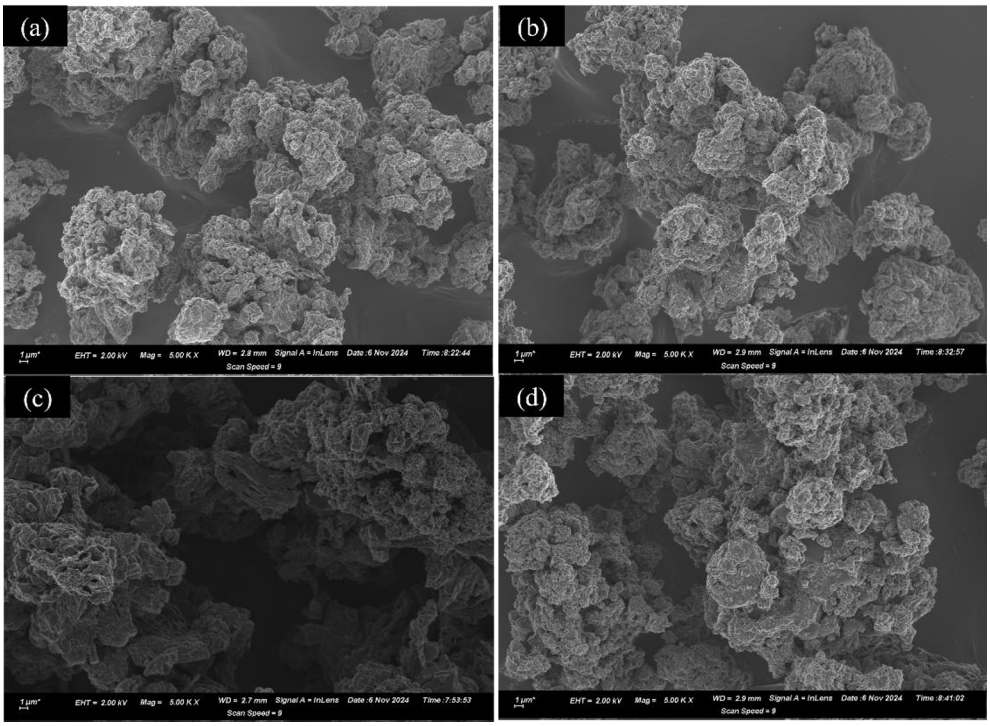

Fig.2. SEM micrographs of (a) PR-S, (b) PR-P, (c) PR-C, (d) PR-N.

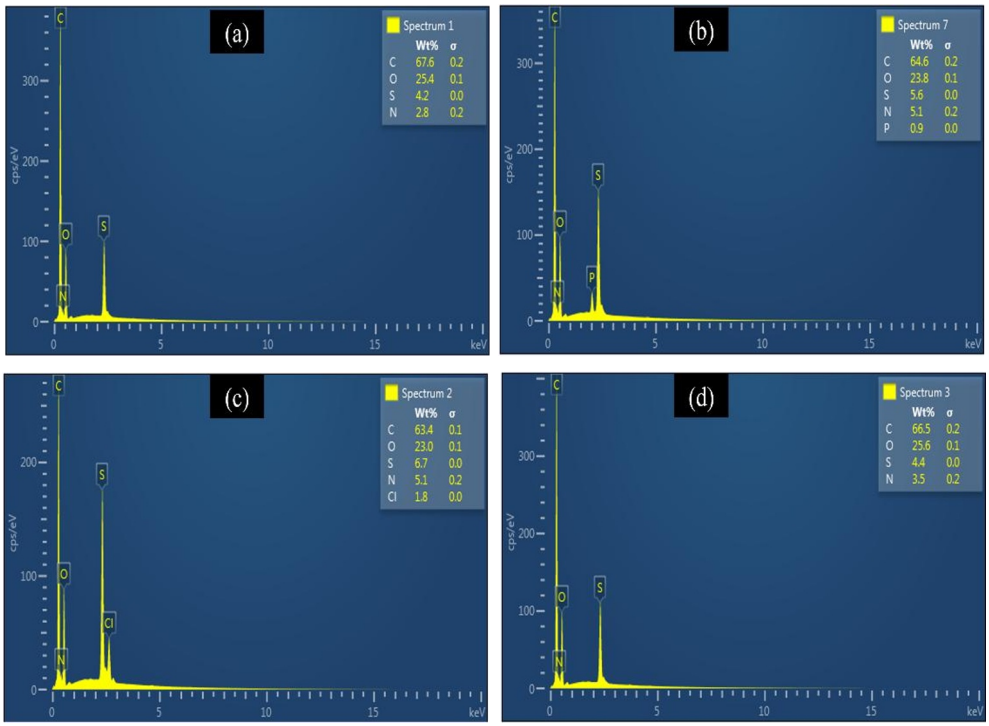

Fig. 3. EDS of (a) PR-S, (b) PR-P, (c) PR-C, and (d) PR-N.

3.3 Electrochemical characterization

The electrochemical properties of PANI/rGO composite electrodes in 1 M $NaSO_4$ electrolyte at potentials between -0.2 and +0.7 V/SCE were investigated. The cyclic voltammetry (CV) was carried out at scan rates from 5 mVs^{-1} to 100 mVs^{-1}. Figure 4a shows the CV curve of the composites at a scan rate of 50 mVs^{-1}. From the curves, all four composites exhibited quasi-rectangular shapes, showing redox peaks with broad cathodic/anodic peaks. This shows that the PANI/rGO composite stores charge via EDLC from rGO and pseudocapacitive behaviour from PANI [15]. PR-C displays the most pronounced redox peaks and the highest current response, which depicts that PR-C enable rapid electronic and ionic transport. Figure 4c shows the CV curve of PR-C at different scan rates (5 - 100 mVs^{-1}). On the other hand, PR-P shows much smaller, broadened peaks, indicating poor redox activity [16]. The current response and the area under the CV curves correspond to the specific capacitance of the electrode material.

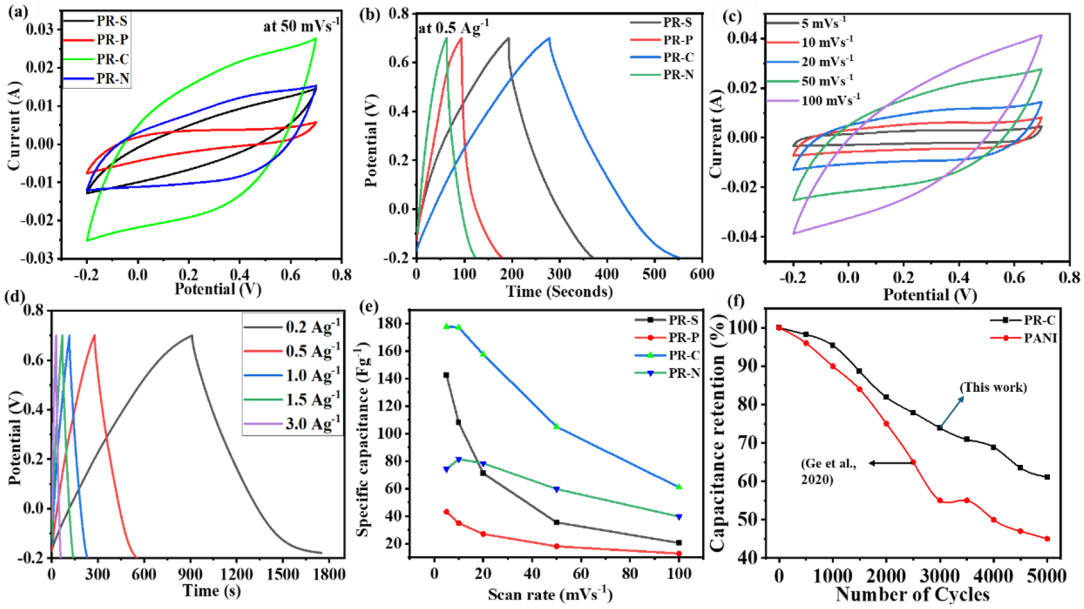

Fig. 4. (a) CV and (b) GCD curves of PANI/rGO composite doped with different inorganic acids at 50mVs^{-1} and 0.5 Ag^{-1}, respectively. (c) CV and (d) GCD curves of PR-C at different scan rates and current densities. (e) Specific capacitance of PR-S, PR-P, PR-C, and PR-N at different scan rates. (f) Capacitance retention of PR-C and pristine PANI.

The galvanostatic charge discharge (GCD) test was done at current density ranging from 0.2 to 3 Ag^{-1} with the voltage window of -0.2V to 0.7V. Figure 4b displays the GCD curves at 0.5 Ag^{-1} for all acid-doped PANI/rGO composites, showing distinct differences across the four dopants. PR-C and PR-S exhibit significantly longer discharge times than PR-P and PR-N, indicating greater charge storage and higher specific capacitance for PR-C and PR-S. All samples display nearly linear voltage–time profiles with minimal curvature, indicating capacitive behaviour and a faradaic process. The discharge slopes correlate with capacitance and internal resistance: PR-C and PR-S have the smallest IR drop, whereas PR-P and PR-N show a high IR drop, indicating higher internal resistance. The specific capacitances of PR-S, PR-P, PR-C and PR-N are 158 Fg^{-1}, 95.4 Fg^{-1}, 207 Fg^{-1}, and 50.3 Fg$^{-1,}$ respectively, and were obtained at a current density of 0.2 Ag^{-1}. Figure 4d reveals the charge-discharge graph of PR-C from current density 0.2 to 3 Ag^{-1}.

The stability study of the PANI/rGO doped with HCl acid was evaluated over 5000 charging and discharging cycles and compared with the stability test of pure PANI, both at 5 Ag^{-1} specific current investigated by Ge and coworkers [17]. Studies have shown that pristine PANI undergoes significant volume swelling, shrinkage, and molecular structural damage during charge-discharge cycles when used as a supercapacitor electrode [18]. This structural instability results in pulverization, degradation of the capacitance and poor cycling performance, limiting its practical application. As shown in Figure 4f, the test reveals that PANI degrades and loses about 45% of its capacitance after just 3000 cycles, whereas PANI/rGO doped with HCl only loses about 38% of its capacitance after 5000 cycles. This superior stability suggests that the PR-C composite can be attributed to rGO effectively restricting PANI's structural deformation and mitigating its swelling and shrinkage effects. The cycling stability of PANI/rGO composites strongly depends on the dopant acid. Fig. 5a shows the cyclic stability of pristine PANI reported by Ge and coworkers and the PANI/rGO doped with different inorganic acids for 5000 cycles. PR-N and PR-P nanocomposite electrodes retain ~ 80% of their initial capacitance, whereas PR-S retains ~72% and HCl-

doped PR-C only ~60%. The difference in the capacitance retention shows that the nature of acid dopants and ion diffusion affects electrochemical stability. Heavier polyatomic anions (e.g., NO_3^-, SO_4^{2-}, $H_2PO_4^-$) are tightly bound within the PANI matrix and reduce structural strain, whereas light anion Cl^- diffuses readily, causing significant volume changes and accelerating the conducting polymer deterioration. This is consistent with a previous report, acid-doped PANI/graphene electrodes with larger or multivalent dopants exhibit excellent durability, maintaining high capacitance retention over thousands of cycles [17].

The electrochemical impedance spectroscopy (EIS) of the composites was investigated to determine the effect of the acid dopants on the PANI/rGO composite on the ionic diffusion and the resistance (Figure 5b). The EIS was performed at an amplitude of 5 mV and a frequency range of 10^{-2} Hz to 10^5 Hz. The open circuit potential (OCP) that was obtained and used for PR-P, PR-S, PR-C, and PR-N measurement was 0.067V, 0.104V, 0.062V, and 0.08V, respectively. According to the Nyquist impedance plot shown in Figure 5b, PR-C exhibits the smallest high-frequency intercept (Rs) and a minimal semicircular arc (Rct), denoting the lowest equivalent series resistance and charge-transfer resistance. PR-S and PR-P show intermediate Rs and Rct, with PR-S slightly lower, reflecting more effective protonation by sulfuric acid relative to phosphoric acid [19]. On the contrary, PR-N displays the largest intercept and semicircle, indicating the highest resistance. The low-frequency region further reveals that PR-C's impedance tail is steepest, indicating a near-ideal capacitive behaviour with efficient ionic diffusion, whereas PR-N curve signifies high Warburg impedance and less ideal capacitance. The EIS result is consistent with the result obtained from the GCD and CV, with the use of strong acid (e.g. HCl and H_2SO_4) as dopants, full protonation is achieved, resulting in improved electronic conductivity and low charge transfer resistance. However, with weak inorganic acid, the internal resistance is high, leading to slower ionic kinetics.

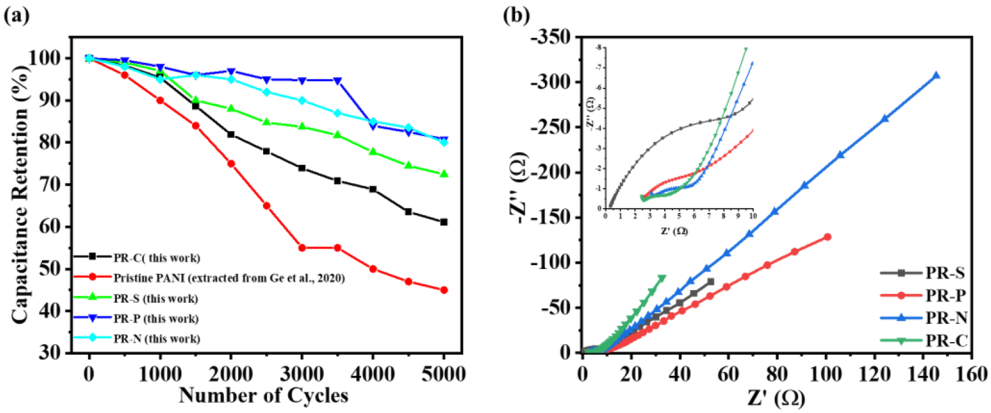

Fig.5. (a) plot of specific capacitance retention of pristine PANI and PANI/rGO composite doped with different inorganic acids. (b) Nyquist plot of PANI/rGO composite doped with different inorganic acids

4 Conclusion

This research focuses on improving the electrochemical properties and cycling stability of PANI-based electrodes to increase the specific capacitance and cyclability of the electrode. PANI/rGO nanocomposites were effectively prepared using in-situ chemical oxidation polymerization using different inorganic acids (HCl, H_2SO_4, H_3PO_4, and HNO_3). Inorganic acid dopants significantly enhance the electrochemical properties of PANI/RGO composites

by protonating PANI chains, thereby improving electrical conductivity and charge transfer kinetics. Dopants enhance a more orderly wrapping of PANI on RGO sheets, which expands the electroactive surface area and promotes ion diffusion. This synergistic interaction of PANI and rGO reduces charge-transfer resistance and boosts cycling stability by mitigating the polymer's inherent swelling/shrinking during redox cycles. Moreover, the presence of rGO also contributes to the enhancement of the electrochemical behaviour of PANI and prevents volumetric instability, which usually results in degradation of the electrode material. PANI/rGO doped with HCl gave the highest electrochemical performance with a specific capacitance of 207 Fg^{-1} at 0.2 Ag^{-1} specific current. This outstanding performance makes PANI/rGO-HCl a potential candidate for supercapacitor application.

References

[1] S. Omar, Z. Ariffin, R. Akhir, D. Shri, M. Halim, M. Safian, H. Azman, R. Ramli,M. Mahat, "Polyaniline (PANI) fabric doped p-toluene sulfonic acid (pTSA) with anti-infection properties," Materials Today: Proceedings, **16**, 1994-2002, (2019), doi: https://doi.org/10.1016/j.matpr.2019.06.083.

[2] A.G. Tabrizi, N. Arsalani, A. Mohammadi, L.S. Ghadimi, I. Ahadzadeh,H. Namazi, "A new route for the synthesis of polyaniline nanoarrays on graphene oxide for high-performance supercapacitors," Electrochimica Acta, **265**, 379-390, (2018), doi: https://doi.org/10.1016/j.electacta.2018.01.166.

[3] O.B. Okafor, A.P.I. Popoola, O.M. Popoola, U.O. Uyor,V.E. Ogbonna, "Review of advances in improving thermal, mechanical and electrochemical properties of polyaniline composite for supercapacitor application," Polymer Bulletin, **81**, 189-246, (2024), doi: https://doi.org/10.1007/s00289-023-04710-y.

[4] J. Ran, Y. Liu, H. Feng, H. Shi,Q. Ma, "A review on graphene-based electrode materials for supercapacitor," Journal of Industrial and Engineering Chemistry, (2024), doi: https://doi.org/10.1016/j.jiec.2024.03.043.

[5] S. Verma, V.K. Pandey,B. Verma, "Facile synthesis of graphene oxide-polyaniline-copper cobaltite (GO/PANI/CuCo2O4) hybrid nanocomposite for supercapacitor applications," Synthetic Metals, **286**, 117036, (2022), doi: https://doi.org/10.1016/j.synthmet.2022.117036.

[6] S. Holla ,M. Selvakumar, "Effect of different electrolytes on the supercapacitor behavior of single and multilayered electrode materials based on multiwalled carbon nanotube/polyaniline composite," Macromolecular Chemistry and Physics, **219**, 1800213, (2018), doi: https://doi.org/10.1002/macp.201800213.

[7] N. Deshpande, S. Chakane,R.R. Borude, "Synthesis and characterization of polyaniline, using different dopant, for sensing application of pollutant gases," J. At. Mol. Condens. Nano Phys, **3**, 27-33, (2016), doi: https://doi.org/10.26713/jamcnp.v3i1.347.

[8] A.H. Navarchian, Z. Hasanzadeh,M. Joulazadeh, "Effect of polymerization conditions on reaction yield, conductivity, and ammonia sensing of polyaniline," Advances in polymer technology, **32**, (2013), doi: https://doi.org/10.1002/adv.21356.

[9] S. Mahalakshmi ,V. Sridevi, "Tailoring the synergy between polyaniline and reduced graphene oxide using organic acid dopant, pTSA for enhanced performance as electrode material for supercapacitor applications," Journal of Physics and Chemistry of Solids, **165**, 110673, (2022), doi: https://doi.org/10.1016/j.jpcs.2022.110673.

[10] S. Abdolhosseinzadeh, H. Asgharzadeh,H. Seop Kim, "Fast and fully-scalable synthesis of reduced graphene oxide," Scientific reports, **5**, 10160, (2015), doi: https://doi.org/10.1038/srep10160.

[11] T. Abdiryim, Z. Xiao-Gang,R. Jamal, "Comparative studies of solid-state synthesized polyaniline doped with inorganic acids," Materials Chemistry and Physics, **90**, 367-372, (2005), doi: https://doi.org/10.1016/j.matchemphys.2004.10.0.

[12] R. Jain, D.K. Sharma,S. Mishra, "High-performance supercapacitor electrode of HNO 3 doped polyaniline/reduced graphene oxide nanocomposites," Journal of Electronic Materials, **48**, 3122-3130, (2019), doi: https://doi.org/10.1007/s11664-019-07048-2.

[13] M.M. Rahman, T. Mahtab, M.Z.B. Mukhlish, M. Faruk,M.M. Rahman, "Enhancement of electrical properties of metal doped polyaniline synthesized by different doping techniques," Polymer Bulletin, **78**, 5379-5397, (2021), doi: https://doi.org/10.1007/s00289-020-03389-9.

[14] H.F. Alesary, H.K. Ismail, A.F. Khudhair,M.Q. Mohammed, "Effects of dopant ions on the properties of polyaniline conducting polymer," Oriental Journal of Chemistry, **34**, 2525, (2018), doi: http://dx.doi.org/10.13005/ojc/340539

[15] F. Ziaeimoghaddam ,R. Arefinia, "Investigation of the effect of doping/dedoping on the redox behavior of polyaniline film: experimental and modeling approach," Progress in Organic Coatings, **170**, 106952, (2022), doi: https://doi.org/10.1016/j.porgcoat.2022.106952.

[16] V. Mane, S. Kale, S. Ubale, V. Lokhande,C. Lokhande, "Enhanced specific energy of silver-doped MnO2/graphene oxide electrodes as facile fabrication symmetric supercapacitor device," Materials Today Chemistry, **20**, 100473, (2021), doi: https://doi.org/10.1016/j.mtchem.2021.100473.

[17] M. Ge, H. Hao, Q. Lv, J. Wu,W. Li, "Hierarchical nanocomposite that coupled nitrogen-doped graphene with aligned PANI cores arrays for high-performance supercapacitor," Electrochimica Acta, **330**, 135236, (2020), doi: https://doi.org/10.1016/j.electacta.2019.135236.

[18] J. Yan, S. Yu, F. Wang, X. Zhang, J. Yang, Q. Guo, L. Huang, J. Liu, Q. Zhang,P.S. Lee, "Long cycle life achieved in polyaniline/SP based self-healing supercapacitor," Electrochimica Acta, **493**, 144394, (2024), doi: https://doi.org/10.1016/j.electacta.2024.144394.

[19] H.M. Abd El-Lateef, M.M. Khalaf, A. Abdou,H. Abd El-Shafy Shilkamy, "Corrosion Inhibition Effect of 2-([(1E)-(2-hydroxyphenyl) methylene] amino) Benzoic Acid on Nickel in Sulfuric Acid: Electrochemical, Charge-Discharge and Computational Studies," ChemElectroChem, **12**, e202400584, (2025), doi: https://doi.org/10.1002/celc.202400584.